

Emergent second law for non-equilibrium steady states

Nahuel Freitas¹ and Massimiliano Esposito¹

¹*Complex Systems and Statistical Mechanics, Department of Physics and Materials Science,
University of Luxembourg, L-1511 Luxembourg, Luxembourg*

(Dated: November 4, 2021)

A long-sought generalization of the Gibbs distribution to non-equilibrium steady states $P_{\text{ss}}(x)$ would amount to relating the self-information $\mathcal{I}(x) = -\log(P_{\text{ss}}(x))$ of microstate x to measurable physical quantities. By considering a general class of stochastic open systems with an emergent deterministic dynamics, we prove that changes in $\mathcal{I}(x)$ along deterministic trajectories can be bounded in terms of the entropy flow Σ_e . This bound takes the form of an emergent second law $\Sigma_e + k_b \Delta \mathcal{I} \geq 0$ which, as we show, is saturated in the linear regime close to equilibrium. A remarkable implication of this result is that the transient deterministic dynamics contains information about the macroscopic fluctuations of non-equilibrium steady states.

PACS numbers:

Introduction. When a system is at equilibrium with its environment (i.e., when no energy or matter currents are exchanged) the probability of a given microstate x is given by the Gibbs distribution [1–3]

$$P_{\text{eq}}(x) = e^{-\beta \Phi(x)} / Z, \quad (1)$$

where $\beta = (k_b T)^{-1}$ is the inverse temperature of the environment, $\Phi(x)$ is the energy of microstate x and $Z = \sum_x \exp(-\beta \Phi(x))$ is the partition function. This is the central result of equilibrium statistical physics, since it has universal validity and connects the microscopic description of a system with the behaviour observed at macroscopic scales (obtained by averaging over microstates according to Eq. (1)). Its relevance in most areas of physics cannot be overstated. A natural question is whether or not a result of similar power and generality also holds for non-equilibrium steady states (NESSs), when a system is subjected to constant flows of energy or matter taking it out of thermal equilibrium. In that case, one can always write the steady state distribution over microstates as

$$P_{\text{ss}}(x) = e^{-\mathcal{I}(x)} \quad (2)$$

in terms of the *self-information* $\mathcal{I}(x)$, also known as fluctuating entropy [4]. In order to provide a useful generalization of the Gibbs distribution to NESSs one must relate the self-information $\mathcal{I}(x)$ to measurable physical quantities. That quest has a long history, starting with the seminal contributions of Lebowitz and MacLennan [5–7] and followed by other works [8–14]. However, it still remains an open problem in non-equilibrium statistical physics, since previous results are either limited to the linear regime close to equilibrium or are not really practical for actual computations. In this Letter we prove, for a very general class of autonomous open systems displaying a macroscopic limit where a deterministic dynamics emerges, the following fundamental bound on self-information changes:

$$\Sigma_a \equiv \Sigma_e + k_b (\mathcal{I}(x_t) - \mathcal{I}(x_0)) \geq 0, \quad (3)$$

where Σ_e is the entropy flow along a *deterministic trajectory* going from microstate x_0 to microstate x_t . For example, in an electronic circuit powered by voltage sources and working at temperature T , the entropy flow is given by $T \Sigma_e = -\int_0^t \dot{Q}(t') dt'$, where $-\dot{Q}$ is the rate of heat dissipation in the resistive elements of the circuit, and can be evaluated from the deterministic dynamics alone. The inequality in Eq. (3) is valid arbitrarily away from thermal equilibrium, and it is saturated in the linear response regime close to equilibrium. Thus, the previous result allows to constraint the steady state distribution over microstates (i.e., the non-equilibrium fluctuations) by only knowing the deterministic dynamics of the system. It is crucial to note (this will become explicit in the derivation below) that Eq. (3) is a stronger statement than the usual second law $\Sigma \equiv \Sigma_e + \Delta S \geq 0$, where ΔS is the system entropy change. Indeed, for deterministic dynamics this latter reduces to just $\Sigma_e \geq 0$, since the system entropy is negligible. This is recovered as a consequence of Eq. (3) by considering the fact that the steady state self-information is a Lyapunov function of the deterministic dynamics [15], which means that $\Delta \mathcal{I} = \mathcal{I}(x_t) - \mathcal{I}(x_0) \leq 0$. Interestingly, one can consider Eq. (3) as the *emergent second law* $\Sigma_e + k_b \Delta \mathcal{I} \geq 0$ where, by comparison with the usual second law, we see that $k_b \Delta \mathcal{I}$ plays the role of the system entropy change. The remarkable feature of this result is that the macroscopic ‘heat’ Σ_e now bounds self-information changes.

Basic setup. To obtain Eq. (3) we will consider stochastic systems, dynamically described by autonomous Markov jump processes, displaying a macroscopic limit in which a deterministic dynamics emerges. Thus, let $\{\mathbf{n} \in \mathbb{N}^k\}$ be the set of possible states of the system, and $\lambda_\rho(\mathbf{n})$ be the rates at which jumps $\mathbf{n} \rightarrow \mathbf{n} + \Delta_\rho$ occur, for $\rho = \pm 1, \pm 2, \dots$ and $\Delta_{-\rho} = -\Delta_\rho$. Thermodynamic consistency is introduced by the *local detailed balance* (LDB) condition [16, 17]. They relate the forward and backward jump rates of a given transition with

the associated entropy production σ_ρ :

$$\sigma_\rho = \log \frac{\lambda_\rho(\mathbf{n})}{\lambda_{-\rho}(\mathbf{n} + \Delta_\rho)} = -\beta [\Phi(\mathbf{n} + \Delta_\rho) - \Phi(\mathbf{n}) - W_\rho(\mathbf{n})]. \quad (4)$$

In the previous equation, $\Phi(\mathbf{n} + \Delta_\rho) - \Phi(\mathbf{n})$ is the energy difference associated to jump ρ , and $W_\rho(\mathbf{n})$ is the non-conservative work provided by external sources during the same jump. For simplicity, we have considered isothermal conditions at inverse temperature β , and therefore the system is taken away from equilibrium by the external work sources alone. More general situations in which a system interacts with several reservoirs at different temperatures can be treated in the same way, this time in terms of a Massieu potential taking the place of $\beta\Phi(\mathbf{n})$ [16]. Important classes of systems accepting the previous description are chemical reaction networks and electronic circuits, which are powered by chemical or electrostatic potential differences, respectively. Note that, by energy conservation, during jump ρ the environment must provide energy $Q_\rho(\mathbf{n}) = \Phi(\mathbf{n} + \Delta_\rho) - \Phi(\mathbf{n}) - W_\rho(\mathbf{n})$, and therefore $\sigma_\rho = -\beta Q_\rho$ is the entropy flow.

The probability distribution $P_t(\mathbf{n})$ over the states of the system at time t evolves according to the master equation

$$\partial_t P_t(\mathbf{n}) = \sum_\rho [\lambda_\rho(\mathbf{n} - \Delta_\rho) P_t(\mathbf{n} - \Delta_\rho) - \lambda_\rho(\mathbf{n}) P_t(\mathbf{n})] \quad (5)$$

From the master equation and the LDB conditions it is possible to derive the energy balance

$$d_t \langle \Phi \rangle = \langle \dot{W} \rangle + \langle \dot{Q} \rangle, \quad (6)$$

and the usual version of the second law:

$$\dot{\Sigma} = \dot{\Sigma}_e + d_t S \geq 0. \quad (7)$$

In the previous equations, $S = -k_b \sum_{\mathbf{n}} P_t(\mathbf{n}) \log(P_t(\mathbf{n}))$ is the Shannon entropy of the system, $\langle \Phi \rangle = \sum_{\mathbf{n}} \Phi(\mathbf{n}) P_t(\mathbf{n})$ is the average energy, and $\dot{\Sigma}_e$ is the entropy flow rate, given by

$$T \dot{\Sigma}_e = -\langle \dot{Q} \rangle = -\sum_{\rho, \mathbf{n}} Q_\rho(\mathbf{n}) j_\rho(\mathbf{n}) \quad (8)$$

where we also defined the heat rate $\langle \dot{Q} \rangle$ in terms of the probability currents $j_\rho(\mathbf{n}) = \lambda_\rho(\mathbf{n}) P_t(\mathbf{n})$ (the work rate $\langle \dot{W} \rangle$ is analogously defined as $\langle \dot{W} \rangle = \sum_{\rho, \mathbf{n}} W_\rho(\mathbf{n}) j_\rho(\mathbf{n})$). The fact that the total entropy production rate is always positive is evident from the following expression due to Schnakenberg [18]:

$$\dot{\Sigma} = \frac{k_b}{2} \sum_{\rho, \mathbf{n}} (j_\rho(\mathbf{n}) - j_{-\rho}(\mathbf{n} + \Delta_\rho)) \log \frac{j_\rho(\mathbf{n})}{j_{-\rho}(\mathbf{n} + \Delta_\rho)} \geq 0. \quad (9)$$

Finally, Eq. (7) can be also expressed as:

$$T \dot{\Sigma} = -d_t F + \langle \dot{W} \rangle \geq 0 \quad (10)$$

where $F = \langle \Phi \rangle - TS$ is the non-equilibrium free energy.

Adiabatic/non-adiabatic decomposition. If the support of $P_t(\mathbf{n})$ can be restricted to a finite subspace of the state space, the Perron-Frobenius theorem states that the master equation in Eq. (5) has a unique steady state $P_{ss}(\mathbf{n})$. Once the steady state is attained, the entropy production rate $\dot{\Sigma}$ matches the entropy flow rate $\dot{\Sigma}_e$. An interesting decomposition of the entropy production rate can be obtained by considering the relative entropy $D = \sum_{\mathbf{n}} P_t(\mathbf{n}) \log(P_t(\mathbf{n})/P_{ss}(\mathbf{n}))$ between the instantaneous distribution $P_t(\mathbf{n})$ and the steady state distribution $P_{ss}(\mathbf{n})$. Then, it is possible to show that $\dot{\Sigma} = \dot{\Sigma}_a + \dot{\Sigma}_{na}$, where

$$\dot{\Sigma}_a = \frac{k_b}{2} \sum_{\rho, \mathbf{n}} (j_\rho(\mathbf{n}) - j_{-\rho}(\mathbf{n} + \Delta_\rho)) \log \frac{j_\rho^{ss}(\mathbf{n})}{j_{-\rho}^{ss}(\mathbf{n} + \Delta_\rho)}, \quad (11)$$

and

$$\begin{aligned} \dot{\Sigma}_{na} &= \frac{k_b}{2} \sum_{\rho, \mathbf{n}} (j_\rho(\mathbf{n}) - j_{-\rho}(\mathbf{n} + \Delta_\rho)) \log \frac{P(\mathbf{n}) P_{ss}(\mathbf{n} + \Delta_\rho)}{P_{ss}(\mathbf{n}) P(\mathbf{n} + \Delta_\rho)} \\ &= -k_b d_t D \end{aligned} \quad (12)$$

are the *adiabatic* and *non-adiabatic* contributions to the entropy production rate $\dot{\Sigma}$, respectively. In Eq. (12) we have introduced the steady state probability currents $j_\rho^{ss}(\mathbf{n}) = \lambda_\rho(\mathbf{n}) P_{ss}(\mathbf{n})$. The non-adiabatic contribution $\dot{\Sigma}_{na}$ is related to the relaxation of the system towards the steady state, since it vanishes when the steady state is reached. This is further evidenced by the identity in the second line of Eq. (12): a reduction in the relative entropy between $P_t(\mathbf{n})$ and $P_{ss}(\mathbf{n})$ leads to a positive non-adiabatic entropy production. The adiabatic contribution $\dot{\Sigma}_a$ corresponds to the dissipation of ‘house-keeping heat’ [19, 20], and at steady state matches the entropy flow rate $\dot{\Sigma}_e$. An important property of the previous decomposition is that both contributions are individually positive: $\dot{\Sigma}_a \geq 0$ and $\dot{\Sigma}_{na} \geq 0$ [21–24]. Thus, the last inequality and the second line in Eq. (12) imply that the relative entropy D decreases monotonically, and since D is positive by definition, it is a Lyapunov function for the stochastic dynamics. The previous two inequalities, in addition to the usual second law $\dot{\Sigma} \geq 0$, have been called the ‘three faces of the second law’ [22]. Also, $\dot{\Sigma}_{na} = -k_b d_t D \geq 0$ was put forward in [25] as an ‘emergent’ second law. There, $\mathcal{F} = k_b D$ was interpreted as an alternative non-equilibrium free energy, with a balance equation $d_t \mathcal{F} = \dot{\Sigma}_a - \dot{\Sigma} \leq 0$ (note the analogy with Eq. (10)). Then, the adiabatic contribution $\dot{\Sigma}_a$ was interpreted as an energy input, which at steady state balances the dissipation $\dot{\Sigma}$. Although this point of view is compelling, it is hindered by the fact that there is not a clear interpretation of $\dot{\Sigma}_a$ away from the steady state, that would allow to compute that quantity in terms of actual physical currents. In this work we take the other possible road, and investigate what are the interpretation and consequences of $\dot{\Sigma}_a \geq 0$.

Emergent second law. We begin by rewriting Eq. (11) using the LDB conditions of Eq. (4) and the definition of \mathcal{I} in Eq. (2), obtaining:

$$\dot{\Sigma}_a = \dot{\Sigma}_e + k_b d_t \langle \mathcal{I} \rangle \geq 0, \quad (13)$$

where we have defined $\langle \mathcal{I} \rangle = \sum_{\mathbf{n}} \mathcal{I}(\mathbf{n}) P_t(\mathbf{n})$ as the average of the steady state self-information $\mathcal{I}(\mathbf{n}) = -\log(P_{ss}(\mathbf{n}))$ computed over the instantaneous distribution. Eq. (13) has been already obtained in [21], although it was not explicitly written in terms of the self-information \mathcal{I} . Note the direct analogy between Eq. (13) and the usual second law in Eq. (7). We see that $d_t \langle \mathcal{I} \rangle$ has taken the place of the (adimensional) system entropy change. Thus, changes in average self-information can be bounded by the entropy flow, that can in turn be computed or measured in terms of actual energy currents (see Eq. (8)). However, the result in Eq. (13) is not yet in an useful form. The reason is that $\langle \mathcal{I} \rangle$ does not depend only on $\mathcal{I}(\mathbf{n})$, the unknown quantity we are interested in, but also on the instantaneous distribution $P_t(\mathbf{n})$, that is also typically unknown except in the few simple cases where the master equation in Eq. (5) can be explicitly solved. The main contribution of this article is to show how Eq. (13) reduces to the useful form in Eq. (3) for systems displaying a macroscopic limit in which a deterministic dynamics emerges, and showing that the inequality is saturated in the linear response regime close to equilibrium. As already mentioned in the introduction, it is important to note that for deterministic dynamics the usual second law in Eq. (7) reduces to $\dot{\Sigma} = \dot{\Sigma}_e \geq 0$, since the system entropy is negligible in the deterministic limit. In contrast, the second law of Eq. (13) remains non-trivial even for deterministic dynamics, relating changes of self-information to the deterministic entropy flow.

Macroscopic limit. In the following we will assume the existence of a scale parameter Ω controlling the size of the system in question. For example, Ω can be taken to be the volume V of the solution in well-mixed chemical reaction networks, or the typical value C of capacitance in the case of electronic circuits. In addition, we will assume that for large Ω i) the transition rates $\lambda_\rho(\mathbf{n})$ are proportional to Ω , ii) that the typical values of the density $\mathbf{x} = \mathbf{n}/\Omega$ remain constant, and iii) that the energy function $\Phi(\mathbf{n} = \Omega\mathbf{x})$ is extensive. Under those conditions, the probability distribution $P_t(\mathbf{x})$ satisfies a large deviations (LD) principle [26–28]:

$$P_t(\mathbf{x}) \asymp e^{-\Omega I_t(\mathbf{x})}, \quad (14)$$

where $I_t(\mathbf{x})$ is a positive time-dependent rate function. Indeed, plugging the previous ansatz in the master equation of Eq. (5) and keeping only the dominant terms in $\Omega \rightarrow \infty$, we see that the $I_t(\mathbf{x})$ evolves according to

$$\partial_t I_t(\mathbf{x}) = \sum_{\rho} \omega_{\rho}(\mathbf{x}) \left[1 - e^{\Delta_{\rho} \cdot \nabla I_t(\mathbf{x})} \right], \quad (15)$$

where $\omega_{\rho}(\mathbf{x}) = \lim_{\Omega \rightarrow \infty} \lambda_{\rho}(\Omega\mathbf{x})/\Omega$ are the scaled jump rates [25, 28]. Also, in the macroscopic limit the LDB

conditions in Eq. (4) take the form

$$\log \frac{\omega_{\rho}(\mathbf{x})}{\omega_{-\rho}(\mathbf{x})} = -\beta [\Delta_{\rho} \cdot \nabla \phi(\mathbf{x}) - W_{\rho}(\mathbf{x})], \quad (16)$$

in terms of the energy density $\phi(\mathbf{x}) = \lim_{\Omega \rightarrow \infty} \Phi(\Omega\mathbf{x})/\Omega$. From Eq. (14) we see that as Ω is increased, $P_t(\mathbf{x})$ is increasingly concentrated around the minimum of the rate function $I_t(\mathbf{x})$, which is the most probable value. Also, deviations from that typical state are exponentially suppressed in Ω . Thus, the limit $\Omega \rightarrow \infty$ is a macroscopic low-noise limit where a deterministic dynamic emerges. In fact, from Eq. (15) one can show that the evolution of the minima \mathbf{x}_t of $I_t(\mathbf{x})$ is ruled by the closed non-linear differential equations

$$d_t \mathbf{x}_t = \mathbf{u}(\mathbf{x}_t) \quad \text{with} \quad \mathbf{u}(\mathbf{x}) = \sum_{\rho} i_{\rho}(\mathbf{x}) \Delta_{\rho}, \quad (17)$$

where the scaled deterministic currents $i_{\rho}(\mathbf{x}) = \omega_{\rho}(\mathbf{x}) - \omega_{-\rho}(\mathbf{x})$ have been introduced [28]. The vector field $\mathbf{u}(\mathbf{x})$ is therefore the deterministic drift in state space. For chemical reaction networks the dynamical equations in Eq. (17) are just the chemical rate equations, while for electronic circuits they are provided by regular circuit analysis.

We can now evaluate the different thermodynamic quantities in the macroscopic limit. For example, to dominant order in $\Omega \rightarrow \infty$, the energy balance in Eq. (6) reads

$$d_t \phi(\mathbf{x}_t) = \mathbf{u}(\mathbf{x}_t) \cdot \nabla \phi(\mathbf{x}_t) = \dot{w}(\mathbf{x}_t) + \dot{q}(\mathbf{x}_t), \quad (18)$$

where the scaled heat and work rates for state \mathbf{x} are defined as $\dot{q}(\mathbf{x}) = \sum_{\rho>0} i_{\rho}(\mathbf{x}) Q_{\rho}(\mathbf{x})$ and $\dot{w}(\mathbf{x}) = \sum_{\rho>0} i_{\rho}(\mathbf{x}) W_{\rho}(\mathbf{x})$, respectively. Note that the entropy flow rate $\dot{\Sigma}_e = -\Omega \dot{q}(\mathbf{x}_t)/T$ is extensive, while in contrast neither the system entropy S nor its derivative $d_t S$ scale with Ω and therefore are negligible in the macroscopic limit. Also to dominant order in $\Omega \rightarrow \infty$, Eq. (11) for the adiabatic entropy production rate $\dot{\Sigma}_a$ reduces to

$$\dot{\Sigma}_a = k_b \Omega [\mathbf{u}(\mathbf{x}_t) \cdot \nabla (I_{ss}(\mathbf{x}) - \beta \phi(\mathbf{x}))|_{\mathbf{x}=\mathbf{x}_t} + \beta \dot{w}(\mathbf{x}_t)], \quad (19)$$

where $I_{ss}(\mathbf{x})$ is the steady state rate function that, according to Eq. (15), satisfies

$$0 = \sum_{\rho} \omega_{\rho}(\mathbf{x}) \left[1 - e^{\Delta_{\rho} \cdot \nabla I_{ss}(\mathbf{x})} \right]. \quad (20)$$

From Eqs. (17), (18) and (19), and the positivity of $\dot{\Sigma}_a$, we find:

$$d_t I_{ss}(\mathbf{x}_t) = \mathbf{u}(\mathbf{x}_t) \cdot \nabla I_{ss}(\mathbf{x}_t) \geq \beta \dot{q}(\mathbf{x}_t), \quad (21)$$

which is the macroscopic version of Eq. (13). Our central result in Eq. (3) is obtained by integrating the previous equation along deterministic trajectories (satisfying Eq. (17)), and noting that the self-information $\mathcal{I}(\mathbf{x})$ and the

steady state rate function $I_{\text{ss}}(\mathbf{x})$ are related by $\mathcal{I}(\mathbf{x}) = \Omega I_{\text{ss}}(\mathbf{x})$, to dominant order in Ω and up to an irrelevant constant.

Linear response regime. We will now show that to first order in the work contributions $W_\rho(\mathbf{x})$ the inequality in Eq. (13) is saturated. In first place we notice, from Eqs. (16) and (20), that in detailed balanced settings (i.e., if $W_\rho(\mathbf{x}) = 0 \forall \rho, \mathbf{x}$) the steady state rate function is just $I_{\text{ss}}(\mathbf{x}) = \beta\phi(\mathbf{x})$, in accordance to the Gibbs distribution. Thus, the difference $g(\mathbf{x}) = I_{\text{ss}}(\mathbf{x}) - \beta\phi(\mathbf{x})$ appearing in Eq. (19) quantifies the deviations from thermal equilibrium. By doing a perturbative analysis of Eq. (20) to first order in $W_\rho(\mathbf{x})$ and $g(\mathbf{x})$, it has been recently shown that

$$\mathbf{u}^{(0)}(\mathbf{x}) \cdot \nabla g(\mathbf{x}) = -\beta\dot{w}^{(0)}(\mathbf{x}) + \mathcal{O}(W_\rho^2), \quad (22)$$

where $\mathbf{u}^{(0)}(\mathbf{x}) = \sum_{\rho>0} i_\rho^{(0)}(\mathbf{x})\Delta_\rho$ and $\dot{w}^{(0)}(\mathbf{x}) = \sum_{\rho>0} i_\rho^{(0)}(\mathbf{x})W_\rho(\mathbf{x})$ are the lowest-order deterministic drift and work rate, respectively [28]. These are defined in terms of the detailed balanced deterministic currents $i_\rho^{(0)}(\mathbf{x}) = \omega_\rho^{(0)}(\mathbf{x}) - \omega_{-\rho}^{(0)}(\mathbf{x})$ constructed from the scaled transition rates evaluated at $W_\rho(\mathbf{x}) = 0$ that, according to the LDB conditions of Eq. (16), satisfy $\log(\omega_\rho^{(0)}(\mathbf{x})/\omega_{-\rho}^{(0)}(\mathbf{x})) = -\beta\Delta_\rho \cdot \nabla\phi(\mathbf{x})$. Comparing the result of Eq. (22) with Eq. (19), we see that $\dot{\Sigma}_a = 0$ to linear order in $W_\rho(\mathbf{x})$. As a consequence, to the same order, the equality is valid in Eqs. (13) and (3). Then, in the linear response regime we can write:

$$\begin{aligned} \mathcal{I}(x_t) - \mathcal{I}(x_0) &\simeq -\beta\Sigma_e^{(0)} \\ &\equiv \beta \left[\phi(x_t) - \phi(x_0) + \int_0^t dt' \dot{w}^{(0)}(\mathbf{x}_{t'}) \right] \end{aligned} \quad (23)$$

where the integration is performed along trajectories solving the detailed balanced deterministic dynamics $d_t \mathbf{x}_t = \mathbf{u}^{(0)}(\mathbf{x}_t)$.

Example. In order to illustrate our results we will consider the model of a low-power complementary metal-oxide semiconductor (CMOS) memory cell developed in [29, 30], that we review in the Supplementary Material. This model involves four MOS transistors and has two degrees of freedom: voltages v_1 and v_2 , that can take values spaced by the elementary voltage $v_e = q_e/C$, where q_e is the positive electron charge and C is a value of capacitance characterizing the device that increases with the scale of the MOS transistors. Thus, in this context the scale parameter can be taken to be $\Omega = V_T/v_e$, where $V_T = k_b T/q_e$ is the thermal voltage. The logical state of the memory is codified in the sign of the variable $x = (v_1 - v_2)/V_T$, and the rate function $I_{\text{ss}}(x)$ associated to the steady state distribution for x can be computed exactly:

$$I_{\text{ss}}(x) = x^2 + 2x \frac{V_{\text{dd}}}{V_T} + \frac{2n}{n+2} [L(x, V_{\text{dd}}) - L(x, -V_{\text{dd}})], \quad (24)$$

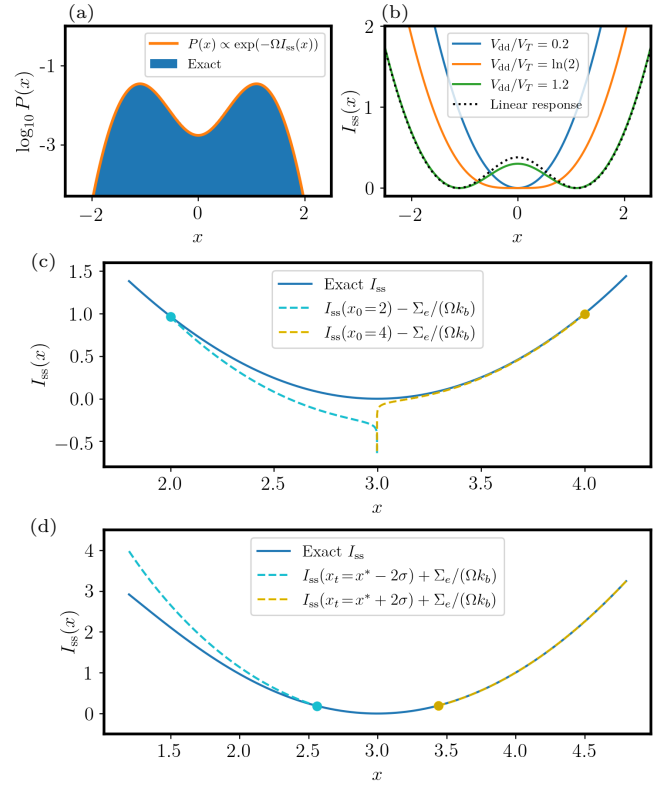


FIG. 1: (a) Comparison between the exact steady state distribution for x and the LD approximation obtained from the rate function $I_{\text{ss}}(x)$ in Eq. (24) ($\Omega = 10$ and $V_{\text{dd}} = 1.2V_T$). (b) Rate function $I_{\text{ss}}(x)$ for different values of the powering voltage V_{dd} . We also compare $I_{\text{ss}}(x)$ with the linear response approximation obtained from Eq. (23) for $V_{\text{dd}} = 1.2V_T$. (c) Illustration of the bound to $I(x_t)$ in Eq. (3) for two different deterministic trajectories starting at $x_0 = 2$ and $x_0 = 4$ ($V_{\text{dd}} = 3V_T$) (d) Bound to $I(x_0)$ for a fixed x_t according to Eq. (3), for $x_t = x^* \pm 2\sigma$ ($\sigma = 1/\sqrt{2\Omega}$, $\Omega = 10$, and $V_{\text{dd}} = 3V_T$).

where V_{dd} is the powering voltage taking the memory out of thermal equilibrium, $L(x, V_{\text{dd}}) = \text{Li}_2(-\exp(V_{\text{dd}}/V_T + x(1 + 2/n)))$, and $\text{Li}_2(\cdot)$ is the polylogarithm function of second order. Also, $n \geq 1$ is a parameter characterizing the transistors (the slope factor).

In Figure 1-(a) we compare the distribution obtained from the previous rate function with exact numerical results. The agreement is essentially perfect even if only a few tens of electrons are involved (the scaling parameter is $\Omega = 10$, and $V_{\text{dd}} = 1.2V_T$). Also, in Figure 1-(b) we show that there is a non-equilibrium transition from a monostable phase into the bistable phase that allows the storage of a bit of information, occurring at the critical powering voltage $V_{\text{dd}}^* = \ln(2)V_T$ for $n = 1$.

We now apply our central result in Eq. (3) and the linear response version of Eq. (23) to the bit model. In Figure 1-(b) we compare the exact rate function in Eq. (24) with the linear response approximation obtained from Eq. (23) for a powering voltage $V_{\text{dd}} = 1.2V_T$,

well into the bistable phase. Remarkably, despite it is only expected to be valid close to equilibrium, the linear response approximation captures the transition to bistability. Finally, in Figure 1-(c) the exact rate function $I_{ss}(x_t)$ along a deterministic trajectory x_t is compared with the lower bound $I_{ss}(x_0) - \Sigma_e(t)/(\Omega k_b)$, for two different trajectories starting at $x_0 = 2$ and $x_0 = 4$. In both cases the trajectory x_t approaches the fixed point $x^* \simeq V_{dd}/V_T = 3$. We see that $I_{ss}(x_0) - \Sigma_e(t)/(\Omega k_b)$ is indeed a lower bound to $I_{ss}(x_t)$, in accordance with Eq. (3). Note that this bound diverges when the trajectory approaches the fixed point x^* . The reason is that once $x_t \simeq x^*$, the entropy flow $\Sigma_e = -(\Omega/T) \int_0^t \dot{q}(x'_t) dt'$ just continuously integrates the steady state heat dissipation rate $-\dot{q}(x^*)$. The linear response approximation avoids this issue since the lowest-order work rate $\dot{w}^{(0)}(x)$ vanishes at the equilibrium fixed point (see Eq. (23)). Alternatively, Eq. (3) can be considered an upper bound to $I(x_0)$ for a fixed final point x_t . This is shown in Figure 1-(d), for final points $x_t = x^* \pm 2\sigma$, where $\sigma = 1/\sqrt{2\Omega}$ estimates the variance of the fluctuations around the fixed point.

For systems accepting a description in terms of Markov jump processes, our results unveil a fundamental connection between the deterministic dynamics that emerges in a macroscopic limit and the non-equilibrium fluctua-

tions at steady state. This has, in addition to its conceptual value, a high practical potential. The reason is that the non-equilibrium fluctuations can typically only be accessed via demanding numerical methods (for example the Gillespie algorithm), while the deterministic dynamics is directly given by the well known network analysis techniques which are for example commonly applied in electronic circuits and chemical reaction networks. Indeed, the corresponding linear response theory, working at the level of the rate function, was shown in [28] to be highly accurate in some model systems from those two fields, with a regime of validity beyond that of usual linear response theories. Our result can also be employed in combination with numerical approaches: once normal or moderately rare fluctuations have been numerically sampled and characterized, Eq. (3) can be used to bound the probability of very rare fluctuations, that otherwise would require extremely long simulation times.

Acknowledgments. We acknowledge funding from the INTER project “TheCirco” (INTER/FNRS/20/15074473) and CORE project “NTEC” (C19/MS/13664907), funded by the Fonds National de la Recherche (FNR, Luxembourg), and from the European Research Council, project NanoThermo (ERC-2015-CoGAgreement No. 681456).

-
- [1] Sheldon Goldstein, Joel L Lebowitz, Roderich Tumulka, and Nino Zanghì. Canonical typicality. *Physical review letters*, 96(5):050403, 2006.
 - [2] Sandu Popescu, Anthony J Short, and Andreas Winter. Entanglement and the foundations of statistical mechanics. *Nature Physics*, 2(11):754–758, 2006.
 - [3] Hans-Otto Georgii. *Gibbs Measures and Phase Transitions*. De Gruyter, Berlin, Germany, May 2011.
 - [4] Udo Seifert. Entropy production along a stochastic trajectory and an integral fluctuation theorem. *Physical review letters*, 95(4):040602, 2005.
 - [5] Joel L Lebowitz and Peter G Bergmann. Irreversible gibbsian ensembles. *Annals of Physics*, 1(1):1–23, 1957.
 - [6] JL Lebowitz. Stationary nonequilibrium gibbsian ensembles. *Physical Review*, 114(5):1192, 1959.
 - [7] James A McLennan Jr. Statistical mechanics of the steady state. *Physical review*, 115(6):1405, 1959.
 - [8] Dmitrii Nikolaevich Zubarev. *Nonequilibrium statistical thermodynamics*. Consultants Bureau, 1974.
 - [9] DN Zubarev. Nonequilibrium statistical operator as a generalization of gibbs distribution for nonequilibrium case. *Cond. Matt. Phys*, 4(7), 1994.
 - [10] Teruhisa S Komatsu and Naoko Nakagawa. Expression for the stationary distribution in nonequilibrium steady states. *Physical review letters*, 100(3):030601, 2008.
 - [11] Christian Maes and Karel Netočný. Rigorous meaning of mclennan ensembles. *Journal of mathematical physics*, 51(1):015219, 2010.
 - [12] Matteo Colangeli, Christian Maes, and Bram Wynants. A meaningful expansion around detailed balance. *Journal of Physics A: Mathematical and Theoretical*, 44(9):095001, 2011.
 - [13] Abhishek Dhar, Keiji Saito, and Peter Hänggi. Nonequilibrium density-matrix description of steady-state quantum transport. *Physical Review E*, 85(1):011126, 2012.
 - [14] H Ness. Nonequilibrium density matrix for quantum transport: Hershfield approach as a mclennan-zubarev form of the statistical operator. *Physical Review E*, 88(2):022121, 2013.
 - [15] Hu Gang. Lyapounov function and stationary probability distributions. *Zeitschrift für Physik B Condensed Matter*, 65(1):103–106, 1986.
 - [16] Riccardo Rao and Massimiliano Esposito. Conservation laws shape dissipation. *New Journal of Physics*, 20(2):023007, feb 2018.
 - [17] Christian Maes. Local detailed balance. *SciPost Phys. Lect. Notes*, 32:1–17, 2021.
 - [18] Jürgen Schnakenberg. Network theory of microscopic and macroscopic behavior of master equation systems. *Reviews of Modern physics*, 48(4):571, 1976.
 - [19] Takahiro Hatano and Shin-ichi Sasa. Steady-state thermodynamics of langevin systems. *Physical review letters*, 86(16):3463, 2001.
 - [20] Thomas Speck and Udo Seifert. Integral fluctuation theorem for the housekeeping heat. *Journal of Physics A: Mathematical and General*, 38(34):L581, 2005.
 - [21] Massimiliano Esposito, Upendra Harbola, and Shaul Mukamel. Entropy fluctuation theorems in driven open systems: Application to electron counting statistics. *Phys. Rev. E*, 76(3):031132, Sep 2007.
 - [22] Massimiliano Esposito and Christian Van den Broeck. Three faces of the second law. I. Master equation formu-

- lation. *Phys. Rev. E*, 82(1):011143, Jul 2010.
- [23] Hao Ge and Hong Qian. Physical origins of entropy production, free energy dissipation, and their mathematical representations. *Phys. Rev. E*, 81(5):051133, May 2010.
 - [24] Riccardo Rao and Massimiliano Esposito. Detailed fluctuation theorems: A unifying perspective. *Entropy*, 20(9):635, 2018.
 - [25] Hao Ge and Hong Qian. Mesoscopic kinetic basis of macroscopic chemical thermodynamics: A mathematical theory. *Physical Review E*, 94(5):052150, 2016.
 - [26] Hugo Touchette. The large deviation approach to statistical mechanics. *Physics Reports*, 478(1-3):1–69, 2009.
 - [27] Hugo Touchette and Rosemary J. Harris. Large deviation approach to nonequilibrium systems. *arXiv*, Oct 2011.
 - [28] Nahuel Freitas, Gianmaria Falasco, and Massimiliano Esposito. Linear response in large deviations theory: a method to compute non-equilibrium distributions. *New Journal of Physics*, 23(9):093003, Sep 2021.
 - [29] Nahuel Freitas, Jean-Charles Delvenne, and Massimiliano Esposito. Stochastic Thermodynamics of Non-Linear Electronic Circuits: A Realistic Framework for Computing around kT. *arXiv (Accepted in PRX)*, Aug 2020.
 - [30] Nahuel Freitas, Karel Proesmans, and Massimiliano Esposito. Reliability and entropy production in non-equilibrium electronic memories. *arXiv*, Mar 2021.

Supplementary material for “Emergent second law for non-equilibrium steady states”

Nahuel Freitas¹ and Massimiliano Esposito¹

¹*Complex Systems and Statistical Mechanics, Department of Physics and Materials Science, University of Luxembourg, L-1511 Luxembourg, Luxembourg*

PACS numbers:

Basic model – We provide here the details of the example given in the main text, based on the model of a non-equilibrium electronic memory developed in [1, 2]. This is a stochastic model of a low-power complementary metal-oxide semiconductor (CMOS) memory cell, whose circuit diagram is shown in Figure 1-(a). This circuit involves two identical CMOS inverters, or NOT gates, connected in a loop. Each inverter is in turn composed of a nMOS transistor and a pMOS transistor. The circuit is subjected to a voltage bias $2V_{\text{dd}}$, and it has two degrees of freedom: the voltages v_1 and v_2 at the output of each inverter. The total electrostatic energy of the full circuit is $\Phi(v_1, v_2) = (C/2)(v_1^2 + v_2^2) + CV_{\text{dd}}^2$, where C is a value of capacitance characterizing the circuit.

Each transistor is modelled as a controlled conduction channel (see details in [1]), and two Poisson rates are associated to conduction events in forward and backward directions. In each conduction event, the voltages $v_{1/2}$ can change by the elementary voltage $v_e = q_e/C$. The Poisson rates can be derived from the I-V curve characterization of the transistors and the local detailed balance conditions [1]. For example, for the pMOS transistor in the first inverter one obtains the following Poisson rates (in subthreshold operation):

$$\begin{aligned}\lambda_+^p(v_1, v_2) &= (I_0/q_e) e^{(V_{\text{dd}} - v_2 - V_{\text{th}})/(nV_T)} \\ \lambda_-^p(v_1, v_2) &= \lambda_+^p(v_1, v_2) e^{-(V_{\text{dd}} - v_1)/V_T} e^{-(v_e/2)/V_T},\end{aligned}\quad (1)$$

In the previous equations, $V_T = k_b T/q_e$ is the thermal voltage and I_0 , V_{th} , and n are parameters characterizing the transistor (respectively known as *specific current*, *threshold voltage*, and *slope factor*). Assuming those parameters are the same for all the transistors, the Poisson rates associated to the nMOS transistor in the first inverter are just $\lambda_{\pm}^n(v_1, v_2) = \lambda_{\pm}^p(-v_1, -v_2)$, while the Poisson rates associated to the transistors in the second inverter are given by $\mu_{\pm}^{n/p}(v_1, v_2) = \lambda_{\pm}^{n/p}(v_2, v_1)$. The total rate for a transition $v_1 \rightarrow v_1 + v_e$ is $A(v_1, v_2) = \lambda_+^p(v_1, v_2) + \lambda_-^n(v_1, v_2)$, and the total rate for a transition $v_1 \rightarrow v_1 - v_e$ is $B(v_1, v_2) = \lambda_-^p(v_1, v_2) + \lambda_+^n(v_1, v_2)$. Then, the state of the system is described by a probability distribution $P(v_1, v_2, t)$ that evolves according to the master equation

$$d_t P(v_1, v_2, t) = PA|_{v_1-v_e, v_2} + PB|_{v_1+v_e, v_2} + PA^*|_{v_1, v_2-v_e} + PB^*|_{v_1, v_2+v_e} - P(A + B + A^* + B^*)|_{v_1, v_2}, \quad (2)$$

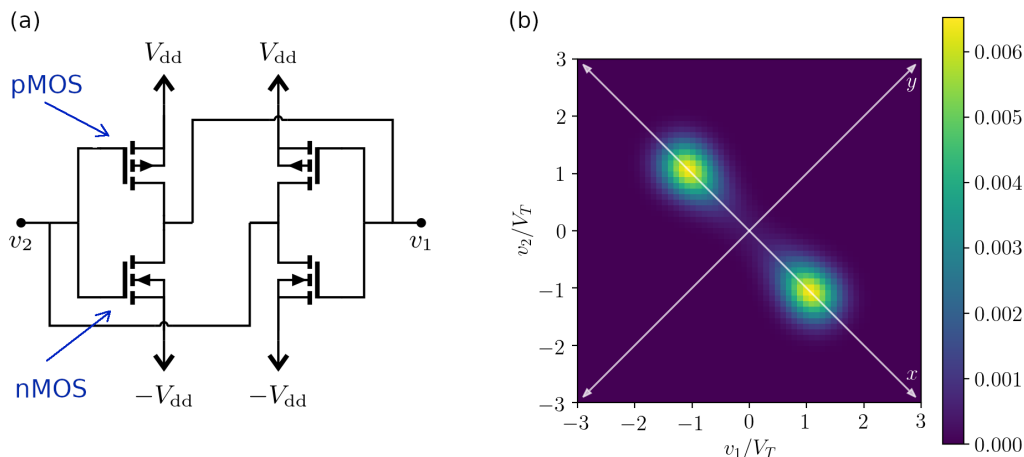


FIG. 1: (a) CMOS implementation of a bistable logical circuit involving two NOT gates in a loop, where each NOT gate is constructed with one pMOS (top) and one nMOS (bottom) transistors. This is the usual way SRAM memory cells are implemented. (b) 2D histogram of the steady state distribution ($V_T = 26$ mV, $v_e/V_T = 0.1$, $V_{\text{dd}}/V_T = 1.2$).

where we are using the compact notation $PA|_{v_1, v_2} = P(v_1, v_2, t)A(v_1, v_2)$, and $A^*(v_1, v_2) = A(v_2, v_1)$. One can numerically compute the steady state distribution from the previous master equation by truncating the state space to a finite number of dimensions. An example is shown in Figure 1-(b).

Macroscopic limit – A macroscopic limit can be introduced by considering a particular scaling of the physical dimensions of the transistors. In a MOS transistor there are two characteristic dimensions defined with respect to the conduction channel [3]: the length L and the width W . For fixed L , both the capacitance C and the characteristic current I_0 increase linearly with W . Thus, we can consider $\Omega = V_T/v_e \propto W$ as the adimensional scale parameter in the main text. In the following we also consider the adimensional voltages v_1 and v_2 , in units of V_T . We also define the scaled rates $a(v_1, v_2) = \lim_{\Omega \rightarrow +\infty} A(v_1, v_2)/\Omega$ and $b(v_1, v_2) = \lim_{\Omega \rightarrow +\infty} B(v_1, v_2)/\Omega$. Then, introducing the large deviations ansatz $P_{ss}(v_1, v_2) \propto \exp(-v_e^{-1}I_{ss}(v_1, v_2))$ in the master equation and keeping only the dominant terms in v_e^{-1} , we obtain the following differential equation for $I_{ss}(v_1, v_2)$:

$$0 = (e^{\partial_{v_1} I_{ss}} - 1) a(v_1, v_2) + (e^{-\partial_{v_1} I_{ss}} - 1) b(v_1, v_2) + (e^{\partial_{v_2} I_{ss}} - 1) a(v_2, v_1) + (e^{-\partial_{v_2} I_{ss}} - 1) b(v_2, v_1). \quad (3)$$

As shown in [2], evaluating the previous equation at $y = v_1 + v_2 = 0$ leads to a differential equation for the reduced rate function $I_{ss}(x)$ associated to the variable $x = v_1 - v_2$ (this is justified by the contraction principle and the fact that the most probable value of y for any value of x is $y = 0$, see Figure 1-(b)). In that way it is possible to derive the expression for $I_{ss}(x)$ given in the main text.

Deterministic dynamics – The deterministic equations of motion for the circuit in Figure 1-(a) read:

$$\begin{aligned} CV_T d_t v_1 &= a(v_1, v_2) - b(v_1, v_2) = i(v_1, v_2) - i(-v_1, -v_2) \\ CV_T d_t v_2 &= a(v_2, v_1) - b(v_2, v_1) = i(v_2, v_1) - i(-v_2, -v_1), \end{aligned} \quad (4)$$

where $i(v_1, v_2) = I_0 e^{(V_{dd}/V_T - V_{th}/V_T - v_2)/n} (1 - e^{-(V_{dd}/V_T - v_1)})$ is the deterministic electric current through the pMOS transistor for given v_1 and v_2 . Alternatively, in terms of variables x and y defined above,

$$\begin{aligned} CV_T d_t x &= i(x, y) - i(-x, -y) - i(-x, y) + i(x, -y) \\ CV_T d_t y &= i(x, y) - i(-x, -y) + i(-x, y) - i(x, -y), \end{aligned} \quad (5)$$

where the change of variables in the functions $a(\cdot, \cdot)$ and $b(\cdot, \cdot)$ is implicit. Noting that $d_t y|_{y=0} = 0$ for all x , we realize that $y(t) = 0$ for all t if we have $y(0) = 0$. This was the case for the deterministic trajectories used to produce Figure 1-(c) in the main text. Finally, we note that the total deterministic work rate for given values of voltages v_1 and v_2 is $\dot{W} = V_{dd}[i(v_1, v_2) + i(-v_1, -v_2) + i(v_2, v_1) + i(-v_2, -v_1)]$. The scaled work rate defined in the main text is in this case $\dot{w} = \dot{W}v_e/V_T$. The detailed balance drift $\mathbf{u}^{(0)}$ and the lowest order work rate $\dot{w}^{(0)}$ are obtained from the previous expressions by evaluating the currents $i(v_1, v_2)$ at $V_{dd} = 0$.

-
- [1] Nahuel Freitas, Jean-Charles Delvenne, and Massimiliano Esposito. Stochastic Thermodynamics of Non-Linear Electronic Circuits: A Realistic Framework for Computing around kT. *arXiv (Accepted in PRX)*, Aug 2020.
- [2] Nahuel Freitas, Karel Proesmans, and Massimiliano Esposito. Reliability and entropy production in non-equilibrium electronic memories. *arXiv*, Mar 2021.
- [3] Yannis Tsididis and Colin McAndrew. *Operation and Modeling of the MOS Transistor*. Oxford Univ. Press, 2011.

